HNPS Advances in Nuclear Physics

Vol 15 (2006)

HNPS2006

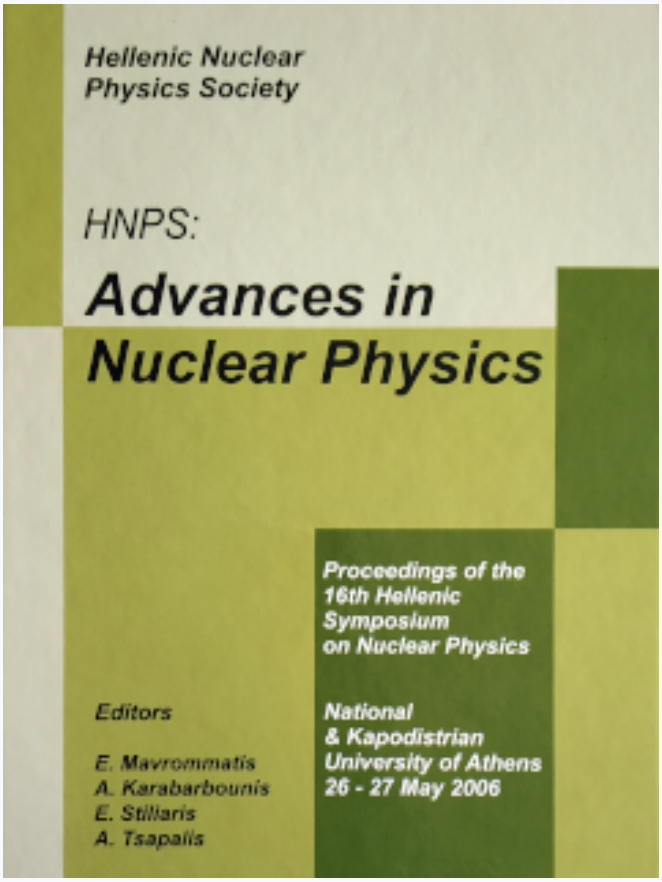

Study of the 191Ir(n,2n)190Ir cross section

N. Patronis, C. T. Papadopoulos, S. Galanopoulos, M. Kokkoris, G. Perdikakis, S. Harissopulos, A. Lagoyannis, R. Vlastou

doi: 10.12681/hnps.2625

Study of the $Ir(n,2n)$ Ir reaction cross section

N. Patronis[a*], C. T. Papadopoulos[a], S. Galanopoulos[a], M. Kokkoris[a], G. Perdikakis[a], S. Harissopulos[b], A. Lagoyannis[b], and R. Vlastou[a]

[a]Department of Physics, National Technical University of Athens

[b]Institute of Nuclear Physics, NCSR "Demokritos", Athens

The ^{191}Ir(n,2n)^{190}Ir cross section was measured by using of the activation technique at four neutron energies in the range 10.0-11.3 MeV. The quasimonoenergetic neutron beam was produced via the ^{2}H(d,n)^{3}He reaction at the 5.5 MV Tandem Van de Graaff accelerator of NCSR "Demokritos". After the irradiations the induced activity of the samples was measured through a 56% relative efficiency HPGe detector. The cross section for the population of the second high spin (11^-) isomeric state was measured along with the sum of the reaction cross section populating both the ground (4^-) and the first isomeric state (1^-). The experimental data will be combared to theoretical calculations in order to deduce information for the spin dependence of the level density parameters.

1. INTRODUCTION

Investigation of neutron threshold reactions, and wherever possible their isomeric cross section ratio, is of considerable interest for testing nuclear models. The prediction of the cross sections for the formation of isomeric states is a difficult task compared to the total reaction channels, since more details on the structure of the residual nucleus have to be taken into account (cf. Ref. [1]). The relative probability of forming isomeric states in a nucleus is mainly governed by the spin state values of the levels involved, and the spin distribution of the excited states of the compound nucleus. The high spin value 11^- of the second isomeric state (m2) of ^{190}Ir (Fig. 1) relative to the corresponding value 4^- of the ground state (g), offers great sensitivity for the study of the spin distribution of the residual nucleus.

The $^{191}Ir(n,2n)$ reaction and the isomeric cross section ratio $\sigma_{m2}/\sigma_{g+m1}$, have been studied in the past at energies higher than 12 MeV (Refs. [2–12]). Furthermore, in these studies limitted information concerning the level scheme of the odd - odd ^{190}Ir [13,14] was available. It should be noted that the details of the level scheme of the residual nuclei [15] are very important to the isomeric cross section ratio calculation, especially in the $^{191}Ir(n,2n)$ reaction, due to the high spin difference between the 11^- isomeric state (m2) and the ground state 4^-.

The purpose of this work was to measure the $^{191}Ir(n,2n)^{190}Ir^{g+m1}$ and $^{191}Ir(n,2n)^{190}Ir^{m2}$ reaction cross section at the neutron beam energy range 10-12 MeV, where no data exist

* lec. r nic a ress: pa. r nis@cen. ral.n. a.gr

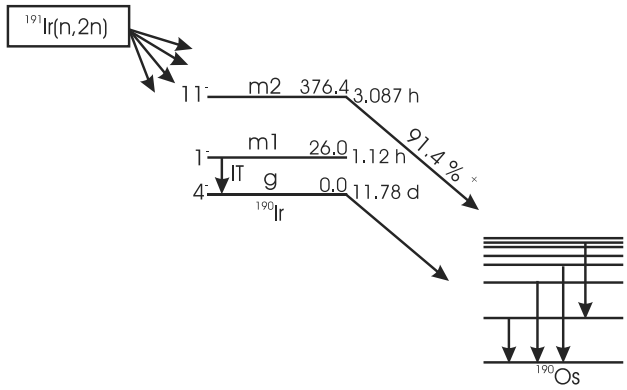

Figure 1. Simplified representation of formation and decay of the ground state and isomeric states of ^{190}Ir. All energies are in keV

in the litarature. Also, theoretical statistical model calculations will be performed in an attempt to investigate spin dependence of the level density as well as the effective moment of inertia of the residual nucleus and their role in the formation of the isomeric state.

2. EXPERIMENTAL

2.1. Irradiations

The $^{191}Ir(n,2n)^{190}Ir$ reaction cross section has been measured at energies 10.0, 10.5, 11.0 and 11.3 MeV, by means of the activation technique. The irradiations were carried out at the 5.5 MV Tandem Van de Graaff accelerator of NCSR "Demokritos". Each irradiation lasted for ∼9 h, corresponding to ∼87 % of the core activity of the second isomeric state (11^-) $^{190}Ir^{m2}$ (Fig. 1). The neutron fluence for the cross section measurement was determined by using the monitor reaction $^{27}Al(n,\alpha)^{24}Na$ as reference [16].

The neutron beam was produced via the $^{2}H(d,n)^{3}He$ reaction, e.g. by bombarding the D_2 gas target [17] with deuteron beam currents, typically kept between 2-6 μA. A 5 μm molybdenum foil served as the entrance window and a Pt foil as the beam stop of the gas cell. During the irradiations the gas target was cooled through a cold air jet, in order to minimize the effect of heating in the deuterium gas pressure, which was continously controlled through a micrometric valve. Using this setup, a flux of the order of $\sim 4 \times 10^6$ n/(cm^2·s) was achieved.

Two natural high purity iridium foils (37.3% ^{191}Ir and 62.7%^{193}Ir) having a diameter of 13 mm, were used for the irradiations. Each 0.5 mm thick sample was placed between identically shaped 0.5 mm thick Al foils. This sample setup was sandwiched once more, between two gold foils, 0.25 mm in thickness and of equal diameter. The neutron flux was deduced from the Al foils, for which the $^{27}Al(n,\alpha)^{24}Na$ reaction cross section is well known. The activity of the Au foils, however, was used for the determination of the

effect of parasitic neutrons to the cross section measurement. The low background of parasitic neutrons from deuteron break up and reactions with the structural materials of the gas target, has been verified experimentally in a previous work [19], by sequential gas-in and gas-out activation experiments as well as by the multiple foil activation technique [20]. These investigations revealed that under certain experimental conditions threshold reaction cross sections can be measured by means of the activation technique, without implementing any correction for the presence of parasitic neutrons. This was also proven from the comparison between the activity of Al and Au foils. The $^{197}Au(n,2n)$ reaction threshold ($E_{thr} = 8.1\ MeV$) and the shape of its excitation function are similar to that of $^{191}Ir(n,2n)$ reaction. Despite the lower threshold ($E_{thr} = 3.2\ MeV$) of the $^{27}Al(n,\alpha)^{24}Na$ reaction, which was finally used as reference, the values of the neutron flux as deduced from Au and Al foils were in excellent agreement. This is a clear indication that the introduced uncertainty due to the presence of parasitic neutrons is negligible compared to other sources of uncertainty.

The neutron flux was monitored by a BF_3 counter placed at 0° with respect to the neutron beam and at a distance of 2 m from the deuteron gas target. The neutron yield, as measured by the BF_3 detector, was recorded at regular time intervals (40 s) by means of a multichannel scaler. This neutron flux history file was used in the analysis, for off-line correction of the fraction of ^{190}Ir nuclei, which had already decayed during activation. The sample sandwich was placed at 0° with respect to the neutron beam and at a distance of 7 cm from the center of the gas cell. At this distance, the angular acceptance of the samples setup was less than ± 5.5°. During the irradiations, the gas cell was constantly operated at a pressure of 1100 mbar, in order to keep the uncertainty of the neutron beam energy distribution, as low as possible.

2.2. Activity measurements

After the irradiations, the induced activity on the samples was measured with a 56 % relative efficiency HPGe detector. The sample to detector distance was more than 10 cm so that any corrections for pile up or coincidence summing effects were negligibly small.

The population of the second isomeric state (m2) was measured independently through the 502 and 616 keV lines of ^{190}Os, where the contribution from the decay of the ground state was small i.e. ∼8% for the 502.5 keV and ∼3% for the 616.5 keV transition. The intensity measurement of these lines, originating from the decay of the 11^- isomeric state, started 2 - 4 hours after the end of the irradiation and lasted for 10 h. The induced activity on the aluminum foils was determined afterwards using the same experimental setup. In less than one hour the activity of the aluminum foils could be determined with a statistical error better than 2 % . The sum of the cross sections for the population of the first isomeric state (m1) and the ground state (g), was determined via the 518.5 keV, 557.9 keV and 569.3 keV transitions of ^{190}Os. These transitions were free from any contribution coming from the decay of the second isomeric state. The measurement of the activity related to the decay of the ground state, started ∼ 16 h after the end of the irradiation to ensure that the 1^- isomeric state (m1) with a half life $T_{1/2} = 1.12\ h$, has fully decayed to the ground state. This procedure was necessary in order to correctly evaluate the sum of the $^{190}Ir^{m1}$ and $^{190}Ir^{g}$ population, since the decay of the first metastable state (m1) is not accompanied by γ emission.

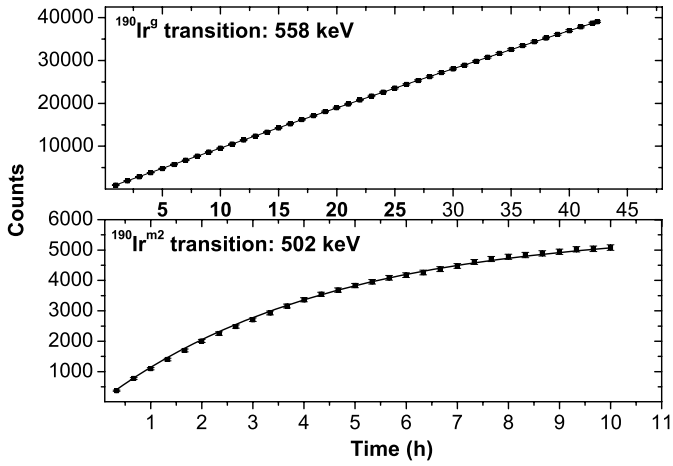

Figure 2. The evolution of the photopeak net area counts with measuring time. The experimental data (points), as resulted after the 10.5 irradiation, are presented with the theoretical fitted curve for the expected half-life time (line). The above panel corresponds to the 558 keV transition from the decay of the ground state (g) and the lower panel to the 502 keV transition form the decay of the second isomeric state (m2).

During the activity measurements the resulted decay spectra of ^{190}Ir were recorded at regular time intervals. By this mean the evolution of the photopeak net area counts with measuring time, could be compared to the theoretical curve for the expected half-life time. As can be seen in Fig. 2 the excellent agreement between the experimental points and the theoretical fitted curve for the expected half-life time, suggest that no contamination was present in the photopeak net area. This procedure was followed for all the used transitions.

3. RESULTS AND DISCUSSION

The experimental results of this work for the $^{191}Ir(n,2n)^{190}Ir^{g+m1}$ and $^{191}Ir(n,2n)^{190}Ir^{m2}$ reactions, as well as the isomeric ratio values are presented in Table 1 along with their uncertainties. All the data reported in this work in the energy range 10 - 12 MeV have been determined for the first time. The only existing data at lower incident neutron energies are at 8.6 MeV and 9.3 MeV [23], where only the sum of the cross section was measured for the population of the ground state (g) and the first isomeric state (m1). In addition, for the$^{191}Ir(n,2n)^{190}Ir$ reaction, the partial cross section for one gamma transition (E_γ=117.3 keV, $6^+ \rightarrow 5^+$), was reported in the past by Fotiades et al. [24].

The cross section data σ_{g+m1} for populating the ground (g) and first isomeric state (m1)

Table 1
Cross sections for the $^{191}Ir(n,2n)^{190}Ir^{g+m1}$ and $^{191}Ir(n,2n)^{190}Ir^{m2}$ reactions

Energy (MeV)	σ_{g+m1} (mb)	σ_{m2} (mb)	$\sigma_{m2}/\sigma_{g+m1}$
10.0	1090±70	25.7±1.6	0.024±0.001
10.5	1400±90	44.4±2.8	0.032±0.002
11.0	1550±100	60.0±3.7	0.039±0.002
11.3	1640±100	65.4±4.0	0.040±0.002

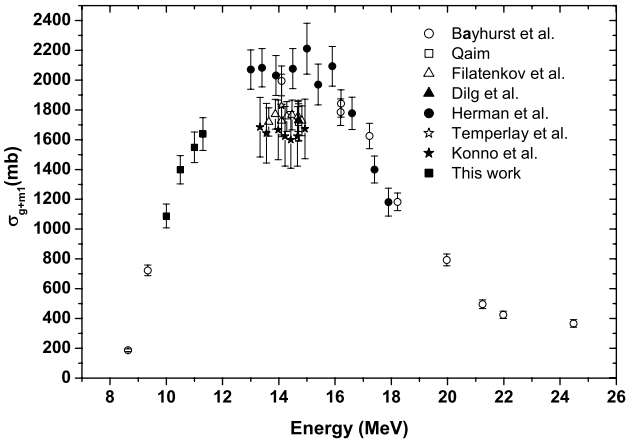

Figure 3. The measured cross section σ_{g+m1} for the population of the ground and first isomeric state of ^{190}Ir

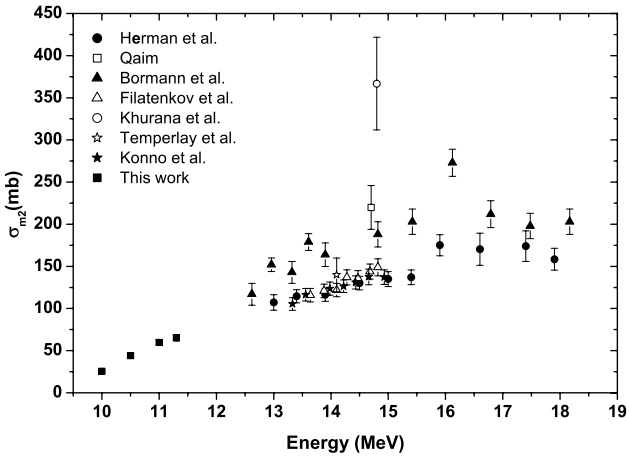

Figure 4. The measured cross section σ_{m2} for the population of the second isomeric state of ^{190}Ir

are shown in Fig. 3 along with all the previous measurements reported in literature. The cross section σ_{m2} of populating the second isomeric state (m2) was measured independently, resulting in the data points presented in Fig. 4. The available experimental cross section data of populating the (m2) metastable state are rather discrepant, particularly in the high neutron beam energy region, where more than one data sets are available.

In the future, statistical model calculations will be performed with emphasis to the reproduction of the available isomeric cross section experimental data. By comparison of the experimental results and the theoretical calculations valuable information can be deduced about the spin dependence of the level density parameters as well as for the role of the level scheme to the isomeric cross section ratio calculation.

4. ACKNOWLEDGMENTS

We thank the Tandem Van de Graaff accelerator crew for the excellent technical assistance. The project is co-funded by the European Social Fund (75 %) and National Resources (25 %) - (EPEAEK - II) - PYTHAGORAS II.

REFERENCES

1. M. Qaim, A. Mushtaq and M. Uhl, Phys. Rev. C 38, 645 (1988)
2. M. Qaim, Nucl. Phys, A185, 614 (1972)
3. M. Herman, A. Marcinkowski and K. Stankiewicz, Nucl. Phys. A430, 69 (1984)
4. C. S. Khurana and H. S. Hans, Nucl. Phys. A28, 560 (1961)

5. Yu. P. Gangrsky, N. N. Kolesnikov, V. G. Lukashik and L. M. Melnikova, Phys. of Atomic Nuclei 67, 1251, (2004)
6. W. Dilg, H. Vonach, G. Winkler and P. Hille, Nucl. Phys. A118, 9 (1968)
7. D. M. Zellermayer and B. Rosner, Phys. Rev. C 6, 315 (1972)
8. A. A. Filatenkov and S. V. Chuvaev, Khlopin Radiev. Inst., Leningrad Reports No. 259, (2003)
9. M. Bormann, H. H. Bissem, E. Magiera and R. Warnemünde, Nucl. Phys. A157, 481 (1970)
10. A. Reggoug and M. Beradda, Nucl. Instrum. Methods Phys. Res. A 255, 107 (1987)
11. C. Konno, Y Ikeda, K. Oishi, K. Kawade, H. Yamamoto and H. Maekawa, JAERI Tokai report series, No. 1329, (1993)
12. J. K. Temperley and D. E. Barnes, Ballistic Research Labs Reports, No. 1491, (1970)
13. C. M. Lederer, Nucl. Data Sheets 35, 525 (1982)
14. B. Singh, Nucl. Data Sheets 61, 243 (1990)
15. B. Singh, Nucl. Data Sheets 99, 275 (2003)
16. The International Reactor Dosimetry File 2002, Nuclear Data Section, IAEA, Vienna
17. G. Vourvopoulos, T. Paradellis and A. Asthenopoulos, Nucl. Instrum. Methods Phys. Res. 220, 23 (1984)
18. H. Klein, H. J. Brede and B. R. L. Siebert, Nucl. Instrum. Methods Phys. Res. 193, 635 (1982)
19. G. Perdikakis, C. T. Papadopoulos, R. Vlastou, A. Lagoyannis, A. Spyrou, M. Kokkoris, S. Galanopoulos, N. Patronis, D. Karamanis, Ch. Zarkadas, G. Kalyva and S. Kossionides, Phys. Rev. C 73, 067601 (2006)
20. R. Vastou et al., J. of Rad. and Nucl. Chem., in press
21. H. Beer and F. Käppeler, Phys. Rev. C 21, 534 (1980)
22. Geant4-Collaboration, the GEANT4 Monte Carlo toolkit for the simulation of the passage of particles through matter, http://wwwinfo.cern.ch/asd/geant4/geant.html
23. B. P. Bayhurst, J. S. Gilmore, R. J. Prestwood, J. B. Wilhelmy, Nelson Jarmie, B. H. Erkkila and R. A. Hardekopf, Phys. Rev. C 12, 451 (1975)
24. N. Fotiades, R. O. Nelson, M. Devlin, M. B. Chadwick, P. Talou, J. A. Becker, P. E. Garrett and W.Younes, Lawrence Livermore National Laboratory, UCRL-PROC-209031, (2005)